48.18, 35.44, 33.31, 31.44, 30.68, 29.33, 29.18, 28.23, 23.03, 21.67, 19.76, 19.62; MS (EI) m/z (relative intensity) 308 (1), 238 (21), 222 (6), 210 (2), 182 (9), 180 (2), 156 (16), 154 (15), 126 (6), 98 (100), 83 (14), 70 (9), 55 (20), 41 (14).

Acknowledgment. N.A.P. thanks NIH (HL17921) and NSF for generous financial support and Professors R. Polniaszek, D. Evans, and D. Curran for helpful discussions at an early stage of the project. B.G. thanks the Swiss National Science Foundation for financial support. D.M.S. and I.J.R. thank the Burroughs Wellcome Fund for receipt of fellowships.

Pentacoordinate 10-Electron Pnictogen–Manganese Adducts: Verification of the 10-Pn-3 Arrangement in ADPnO Molecules

Anthony J. Arduengo, III,* Michael Lattman,† H. V. Rasika Dias, Joseph C. Calabrese, and Michael Kline

Contribution No. 5589 from the Central Research and Development Department, E. I. du Pont de Nemours & Company, Experimental Station, Wilmington, Delaware 19880-0328.
Received September 6, 1990

Abstract: The bis(cyclopentadienylmanganese dicarbonyl) complexes of 5-aza-2,8-dioxa-1-pnictabicyclo[3.3.0]octa-2,4,6-triene (ADPnO) molecules have been prepared and structurally characterized for arsenic and antimony. These complexes represent the first demonstration of chemical reactivity for both pnictogen lone pairs of electrons in ADPnO molecules. In the case of the phosphorus system (ADPO) only a monoadduct is obtained. The ADPO·$Mn(Cp)(CO)_2$ adduct exhibits a tetracoordinate 8-electron arrangement at phosphorus. These results support the 10-Pn-3 designations previously assigned to the ADPnO molecules and are in accord with recent theoretical models. Comparisons are made with pnictinidene bis(metal) complexes as well as 5-coordinated antimony derivatives of ADSbO.

Introduction

In previous reports we have described the synthesis,[1-5] structure,[1-4] chemistry,[1-4,6-11] and electronic structure[4,11] of unusual ring systems that contain 3-coordinate 10-electron pnictogen centers (10-Pn-3;[12] Pn ≡ pnictogen = P, As, Sb). Theoretical studies[4,11] on these ADPnO[13] ring systems have indicated that the arsenic and antimony compounds are adequately described by a simple valence bond model such as **1a**. This model places two

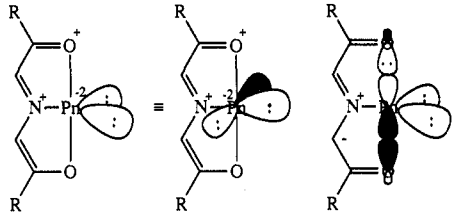

1a **1b**

lone pairs of electrons in equatorial sites of the idealized pseudo-trigonal-bipyramidal (Ψ-TBP) geometry at the pnictogen center. It is also possible to represent these lone pairs of electrons as a σ and π set rather than an equivalent set of approximate sp^2 hybridized orbitals.

The theoretical models of the phosphorus-derived ADPO system show characteristics similar to the heavier arsenic and antimony analogues.[4,11] However, because the size of the phosphorus is closer to those of the neighboring nitrogen and oxygen atoms, overlap between these centers is sufficient to allow delocalization of one phosphorus lone pair into the ligand backbone. This loss of electron density from phosphorus is not sufficient to cause a change in the ground-state structure to the more conventional folded 8-P-3 arrangement. Since the phosphorus center of ADPO remains in a planar T-shaped geometry, the designation of "10-P-3 ADPO" can still be applied semantically. Nonetheless, it is important to remember that the phosphorus π lone pair in 10-P-3 ADPO is delocalized and the 8-P-3 and 10-P-3 arrangements are close in energy: a fact that is reflected in ADPO's coordination chemistry.[4,6,10]

A description of the bonding in the ADPnO molecules in which the pnictogen center is viewed as an internally solvated pnictinidene (6-Pn-1) center has been discussed.[11] Structure **1b** depicts a pnictinidene center that is internally solvated by the carbonyl substituents of an azomethine ylide. As we have discussed previously, the pnictogen–oxygen interaction in the ADPnO molecules is too strong to be regarded as mere solvation. Although an exaggeration, the pnictinidene model of the ADPnO molecules does provide insight. With this view of these bonding systems in mind, it is useful to recall reports of pnictinidene bis(metal) complexes[14-28] (**2**), which can serve as reference points for

† Visiting Research Scientist on leave from the Department of Chemistry, Southern Methodist University, Dallas, TX 75275.

(1) Culley, S. A.; Arduengo, A. J., III *J. Am. Chem. Soc.* **1984**, *106*, 1164.
(2) Culley, S. A.; Arduengo, A. J., III *J. Am. Chem. Soc.* **1985**, *107*, 1089.
(3) Stewart, C. A.; Harlow, R. L.; Arduengo, A. J., III *J. Am. Chem. Soc.* **1985**, *107*, 5543.
(4) Arduengo, A. J., III; Stewart, C. A.; Davidson, F.; Dixon, D. A.; Becker, J. Y.; Culley, S. A.; Mizen, M. B. *J. Am. Chem. Soc.* **1987**, *109*, 627.
(5) Arduengo, A. J. U. S. Patent 4710576, 1987.
(6) Arduengo, A. J., III; Stewart, C. A.; Davidson, F. *J. Am. Chem. Soc.* **1986**, *108*, 322.
(7) Stewart, C. A.; Arduengo, A. J., III *Inorg. Chem.* **1986**, *25*, 3847.
(8) Arduengo, A. J., III *Pure Appl. Chem.* **1987**, *59*, 1053.
(9) Arduengo, A. J., III; Dixon, D. A.; Stewart, C. A. *Phosphorus, Sulfur Relat. Elem.* **1987**, *30*, 341.
(10) Arduengo, A. J., III; Lattman, M.; Calabrese, J. C.; Fagan, P. J. *Heteroat. Chem.* **1990**, *1*, 407.
(11) Arduengo, A. J., III; Dixon, D. A. Electron Rich Bonding at Low Coordination Main Group Element Centers. In *Heteroatom Chemistry*; ICHAC-2; Block, E., Ed.; VCH: New York, 1990; p 47.
(12) The *N-X-L* nomenclature system has been previously described: Perkins, C. W.; Martin, J. C.; Arduengo, A. J., III; Lau, W.; Algeria, A.; Kochi, J. K. *J. Am. Chem. Soc.* **1980**, *102*, 7753. *N* valence electrons about a central atom *X*, with *L* ligands.
(13) The ADPnO acronym has been previously described and is used for simplicity in place of the name of the ring system it represents: 5-*aza*-2,8-*dioxa*-1-*pnictabicyclo*[3.3.0]*octa*-2,4,6-triene. See ref 4, footnote 1d for details.
(14) Arif, A. M.; Cowley, A. H.; Norman, N. C.; Orpen, A. G.; Pakulski, M. *Organometallics* **1988**, *7*, 309.
(15) Bartlett, R. A.; Dias, H. V. R.; Flynn, K. M.; Hope, H.; Murray, B. D.; Olmstead, M. M.; Power, P. P. *J. Am. Chem. Soc.* **1987**, *109*, 5693.

0002-7863/91/1513-1799$02.50/0

ADPnO–metal chemistry.

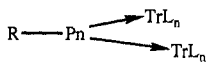

2

Pn = pnictogen (P, As, Sb)
Tr = transition metal

The transition-metal coordination chemistry of the ADPnO molecules has played a central role in understanding the nature of the bonding in these unusual molecules.[4,6,7,10] For ADAsO and ADSbO, the metal adducts are formed by employing a lone pair from the heavy pnictogen center in a coordinative covalent bond with the transition-metal center. The presence of a second lone pair of electrons at the central pnictogen can be inferred from the geometry of the pnictogen center and the electron count associated with the tridentate organic ligand backbone (which is unchanged upon complexation). These ADPnO–metal adducts can be represented by structure **3**. Previous work has demonstrated the chemical reactivity of only one pnictogen lone pair in the ADPnO molecules. There has been some suggestion that the second lone pair at the antimony center of an ADSbO·Ru complex exhibits some reactivity in substitution reactions.[10] In contrast to the pnictinidene bis(metal) adducts, **2**, previously only mono-adducts between ADPnO molecules and transition-metal electrophiles have been obtained. Even though the chemical reactivity of both pnictogen lone pairs has not been proven experimentally, there is ample structural evidence for the presence of stereochemically active lone pairs in ADAsO and ADSbO metal adducts and oxidative addition products.[2-4,7-10]

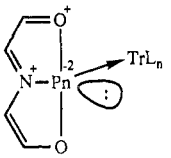

3

Pn = As, Sb

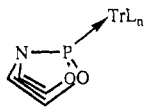

4

In contrast to its heavier analogues, ADPO exhibits coordination chemistry and oxidative addition chemistry that reflects the closer relationship between the 10-P-3 (planar) and 8-P-3 (folded) forms of this phosphorus molecule. As such, the transition-metal adducts of ADPO have all shown the folded geometry of the ADPO ring, which is depicted by structure **4**. The electronic and steric factors that favor this coordination mode for ADPO have been described.[10]

We now report new coordination chemistry for the ADPnO molecules that demonstrates chemical reactivity of both lone pairs at arsenic and antimony centers and provides the first examples of bridging coordination of a 3-coordinate pnictogen ligand. The ADPO coordination chemistry reported herein provides further support for the previous models of the bonding in ADPO.

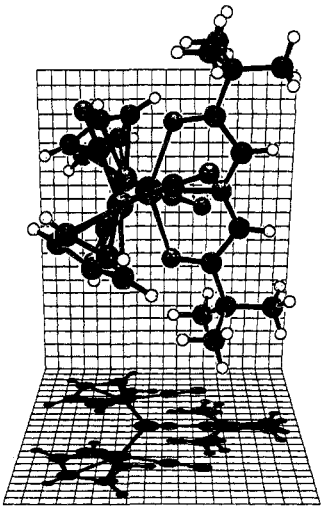

Figure 1. KANVAS[31] drawing of ADSbO·$[MnCp(CO)_2]_2$.

Results

The reaction of ADSbO with 2 equiv of $MnCp(CO)_2$·THF in THF yields the 2:1 adduct ADSbO·$[MnCp(CO)_2]_2$ (eq 1).

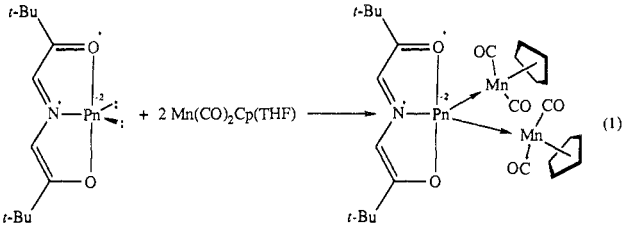

(1)

ADPnO **ADPnO·$[MnCp(CO)_2]_2$**

Pn = Sb, As

ADSbO·$[MnCp(CO)_2]_2$ forms dark green crystals [mp 218–220 °C (dec)], insoluble in hexane, readily soluble in THF and dichloromethane. The IR spectrum of ADSbO·$[MnCp(CO)_2]_2$ in THF displays two pronounced absorptions (the band at higher frequency shows a shoulder) in the ν_{CO} region. These absorptions [1865 (vs), 1919 (vs), 1932 (sh) cm^{-1}] suggest that there may be only a very low rotational barrier about the Sb–Mn bond.[29] The IR spectra of the related phenylstibinidene bis($MnCp(CO)_2$) complex is somewhat more complex, indicating rotameric equilibria.[16,27,28] As expected, the ^{13}C NMR spectrum of ADSbO·$[MnCp(CO)_2]_2$ in CH_2Cl_2 shows only a single resonance at δ 229.3 for the metal-bound carbonyls, indicating equivalent carbonyls on the NMR time scale. The 2:1 stoichiometry of ADSbO·$[MnCp(CO)_2]_2$ is confirmed by the integrals in the ^1H NMR spectrum and the elemental analysis. Both the ^1H and ^{13}C NMR spectra of ADSbO·$[MnCp(CO)_2]_2$ (Table I) are consistent with electronic and structural arrangements similar to those of non-complexed ADSbO.[3,4]

The structure of ADSbO·$[MnCp(CO)_2]_2$ was determined by single-crystal X-ray diffraction and is illustrated in Figure 1. Selected bond distances and angles are listed in Tables II and III, along with corresponding parameters for reference molecules.[30]

(16) Huttner, G.; Evertz, K. *Acc. Chem. Res.* **1986**, *19*, 406.
(17) Lang, H.; Huttner, G.; Jibril, I. *Z. Naturforsch.* **1986**, *41B*, 473.
(18) Hinke, A.-M.; Hinke, A.; Kuchen, W.; Hönle, W. *Z. Naturforsch.* **1986**, *41B*, 629.
(19) Lang, H.; Orama, O.; Huttner, G. *J. Organomet. Chem.* **1985**, *291*, 293.
(20) Weber, U.; Zsolnai, L.; Huttner, G. *J. Organomet. Chem.* **1984**, *260*, 281.
(21) Huttner, G.; Borm, J.; Zsolnai, L. *J. Organomet. Chem.* **1984**, *263*, C33.
(22) Herrmann, W.; Koumbouris, B.; Zahn, T.; Ziegler, M. L. *Angew. Chem., Int. Ed. Engl.* **1984**, *23*, 812.
(23) Jones, R. A.; Whittlesey, B. R. *Organometallics* **1984**, *3*, 469.
(24) Flynn, K. M.; Murray, B. D.; Olmstead, M. M.; Power, P. P. *J. Am. Chem. Soc.* **1983**, *105*, 7060.
(25) Sigwarth, B.; Zsolnai, L.; Scheidsteger, O.; Huttner, G. *J. Organomet. Chem.* **1982**, *235*, 43.
(26) von Seyerl, J.; Sigwarth, B.; Schmid, H.; Mohr, G.; Frank, A.; Marsili, M.; Huttner, G. *Chem. Ber* **1981**, *114*, 1392.
(27) von Seyerl, J.; Huttner, G. *Angew. Chem., Int. Ed. Engl.* **1978**, *17*, 843.
(28) von Seyerl, J.; Moering, U.; Wagner, A.; Frank, A.; Huttner, G. *Angew. Chem., Int. Ed. Engl.* **1978**, *17*, 844.
(29) Strohmeier, V. W.; Guttenburger, J. F.; Hellmann, H. *Z. Naturforsch.* **1964**, *19B*, 353.
(30) The structural data on previously reported compounds were obtained directly from the referenced work or from the Cambridge Structural Database; see: Allen, F. H.; Bellard, S. A.; Brice, M. D.; Cartwright, B. A.; Doubleday, A.; Higgs, H.; Hummelink, T.; Hummelink-Peters, B. G.; Kennard, O.; Motherwell, W. D. S.; Rodgers, J. R.; Watson, D. G. *Acta Crystallogr.* **1979**, *B35*, 2331. Allen, F. H.; Kennard, O.; Taylor, R. *Acc. Chem. Res.* **1983**, *16*, 146.

Table I. Selected Chemical Shifts (δ) in ADPnO Molecules and Their Mn and Halogen Adducts

compound	^{1}H				^{13}C					^{31}P	ref
	t-Bu	HCN	Cp	C_3C	C_3C	CN	COPn	C≡O	Cp		
$ADSbO{\cdot}[MnCp(CO)_2]_2$	1.31	8.08	4.50	27.6	41.0	119.9	196.5	229.3	79.7		this work
$ADAsO{\cdot}[MnCp(CO)_2]_2$	1.32	7.80	4.49	27.4	40.3	118.7	191.5	231.1	81.7		this work
$ADPO{\cdot}MnCp(CO)_2$	1.12	5.74	4.62	27.4	32.5	113.3	155.2	228	81.7	256	this work
ADASbO	1.39	8.46		28.8	38.0	117.8	176.6				4
ADAsO	1.31	7.90		28.3	36.3	113.6	174.8				4
ADPO	1.31	7.50		28.1	34.3	111.2	169.9			187	4
$ADSbO{\cdot}Cl_2$	1.38	7.94		27.0	41.0	119.3	202.9				4
$ADSbO{\cdot}I_2$	1.36	8.12		26.6	41.3	121.8	203.8				this work
$ADAsO{\cdot}Cl_2$	1.35	7.70		26.6	40.3	121.2	196.7				4
$[(ADSbO)_3{\cdot}Ru(C_5(CH_3)_5)]^+$	1.30	8.74		28.4	40.4	124.3	190.1				10
$[ADSbO{\cdot}PtCH_3(P(C_6H_5)_3)_2]^+$	1.43	8.72		27.9	41.1	123.9	195.6				7

Table II. Selected Bond Lengths (pm) in $ADPnO{\cdot}[Mn(CO)_2Cp]_2$ and Reference Molecules[30]

compound	Pn–N	Pn–O	N–C	NC–CO	C–OPn	Pn–Mn	MnC–O	Mn–$Cp_{(cent.)}$	ref
$ADSbO{\cdot}[Mn(CO)_2Cp]_2$	223.4 (6)	225.4 (4)	132.6 (5)	140.7 (7)	127.4 (6)	245.8 (0)	116.5[a]	176.5	this work
$ADAsO{\cdot}[Mn(CO)_2Cp]_2$	204.3 (2)	216.0 (1)	134.0 (2)	141.6 (3)	126.1 (2)	231.2 (0)	115.6[a]	177.2	this work
$ADPO{\cdot}MnCp(CO)_2$	172.9 (2)	163.8[a]	143.0[a]	131.5[a]	141.5[a]	212.6 (0)	115.4[a]	176.7	this work
ADSbO	206.4	215.5[a]	135.0[a]	137.3[a]	132.0[a]				4
ADAsO	183.9	197.7[a]	137.3[a]	136.3[a]	130.9[a]				4
$C_6H_5{-}Sb{\cdot}[Mn(CO)_2Cp]_2$[b]						245.7[a]	[c]	[c]	27
$C_6H_5{-}As{\cdot}[Mn(CO)_2Cp]_2$[b]						227.0[a]	119.2[a]	179.0	26
$(C_6H_5)_3P{\cdot}Mn(CO)_2Cp$						223.6	117.0[a]	177.6	32
$ADSbO{\cdot}Cl$	220.0[a]	220.0[a]	132.8[a]	141.0[a]	128.3[a]	253.7[a,d]			4
$ADSbO{\cdot}I_2$	218.0	222.0[a]	131.5[a]	143.0[a]	125.0[a]	295.1[a,d]			this work
$[(ADSbO)_3{\cdot}Ru(CH_3)_5)]^+$	214.9[a]	220.2[a]	135.3[a]	139.0[a]	129.0[a]	259.1[a,e]			10
$[ADSbO{\cdot}PtCH_3(P(C_6H_5)_3)_2]^+$	210.3	217.7[a]	137.0[a]	137.5[a]	129.0[a]	264.1[f]			7

[a] Chemically equivalent but crystallographically unique distances have been averaged. [b] Each manganese center is crystallographically unique. [c] Insufficient data were reported to calculate this value. [d] This datum is for the antimony–halogen distance. [e] This datum is for the antimony–rhenium distance. [f] This datum is for the antimony–platinum distance.

Table III. Selected Angles (deg) in $ADPnO{\cdot}[Mn(CO)_2Cp]_2$ and Reference Molecules[30]

compound	O–Pn–O	N–Pn–O	C–O–Pn	C–N–Pn	C–C–N	C–C–O	C–N–C	Mn–Pn–Mn	NPn–$MnCp_{(cent.)}$	ref
$ADSbO{\cdot}[Mn(CO)_2Cp]_2$	142.7 (2)	71.3 (1)	116.4 (3)	116.6 (3)	116.3 (5)	119.2 (5)	126.7 (7)	141.3 (0)	113.1	this work
$ADAsO{\cdot}[Mn(CO)_2Cp]_2$	151.0 (0)	75.5 (0)	114.5 (1)	117.0 (1)	115.0 (2)	117.9 (2)	126.0 (2)	136.6 (0)	14.6	this work
$ADPO{\cdot}MnCp(CO)_2$	109.5 (0)	94.0[a]	111.0[a]	106.7[a]	114.5[a]	113.1[a]	116.0 (2)		79.6	this work
ADSbO	149.6	74.8[a]	114.7[a]	117.5[a]	115.8[a]	117.2[a]	125.1			4
ADAsO	160.3	80.2[a]	114.2[a]	117.4[a]	113.2[a]	115.1[a]	125.2			4
$C_6H_5{-}Sb{\cdot}[Mn(CO)_2Cp]_2$[b]								140.0	[c]	27
$C_6H_5{-}As{\cdot}[Mn(CO)_2Cp]_2$[b]								138.3	5.6, 179.9	26
$ADSbO{\cdot}Cl_2$	145.7[a]	72.9[a]	116.0[a]	116.2[a]	115.7[a]	119.2[a]	127.7[a]	158.6[a,d]		4
$ADSbO{\cdot}I_2$	145.1	72.6[a]	116.0[a]	116.5[a]	116.0[a]	118.5[a]	127.0	160.6[d]		this work
$[(ADSbO)_3{\cdot}Ru(C_5(CH_3)_5)]^+$	145.3[a]	72.7[a]	115.4[a]	117.9[a]	114.0[a]	119.8[a]	123.7[a]			10
$[ADSbO{\cdot}PtCH_3(P(C_6H_5)_3)_2]^+$	146.2	73.3[a]	119.9[a]	118.0[a]	112.5[a]	119.5[a]	123.0			7

[a] Crystallographically unique but chemically equivalent angles have been averaged. [b] Each manganese center is unique. [c] Insufficient data were reported to calculate this value. [d] This datum is actually the halogen–antimony–halogen angle. Halogens are bent toward the ligand, as in the drawings.

The geometry about the antimony is best described as a distorted trigonal bipyramid (TBP) with the oxygens at axial positions and the nitrogen and two manganese atoms occupying the equatorial sites. The trigonal aspect of the geometry is readily apparent from the shadow cast on the lower plane in Figure 1. The tridentate organic ligand that is bonded to the antimony center shows the planar geometry that would be expected for an electronic arrangement similar to that in noncomplexed ADSbO. The $C{-}C_{ring}$ bond in the tridentate ligand has lengthened relative to ADSbO while the C–O and C–N bonds have both shortened. The ring internal angles at the oxygen and carbons increase relative to ADSbO. The ring internal angles at antimony and nitrogen both decrease relative to ADSbO. These changes are similar to the ones observed upon the formation of the 5-coordinated $ADSbO{\cdot}X_2$ compounds.[4] Consistent with the angle changes, there is an 8.2% increase in the Sb–N bond length along with a 4.6% increase in the Sb–O bond lengths upon complexation to the manganese centers. The result of these changes is that the antimony appears to be "pulled out" of the tridentate ligand by the manganese centers. The antimony lies exactly in the plane defined by the three equatorial atoms. The Mn–Sb–Mn angle of 141.25° is significantly larger than the 120° that would be expected for an exact TBP geometry but is very similar to the 140° angle reported for $C_6H_5Sb{\cdot}[MnCp(CO)_2]$.[27] The Sb–Mn bond length in $ADSbO{\cdot}[MnCp(CO)_2]_2$ is also very similar to Sb–Mn distances found in stibinidene bis(metal) complexes.[20,27] A particularly noteworthy feature of the structure of $ADSbO{\cdot}[MnCp(CO)_2]_2$ is the 113.1° dihedral angle calculated for $N{-}Sb{-}Mn{-}Cp_{(centroid)}$. As can be seen from the direct view in Figure 1, this places the Cp substituents on the opposite side of the antimony from the tridentate ligand. However, the Cp groups are 66.9° away from being antiperiplanar to the Sb–N bond. This disposition of the Cp groups is striking when compared to the stibinidene bis(metal) complexes, which characteristically have values near either 0° of 180° for the related dihedral angles (vide infra).

Although we have previously observed that ADAsO and ADSbO show different reactivity toward the ruthenium-centered electrophile, $[RuCp^*]^+$,[10] the reactions with $MnCp(CO)_2$ follow similar courses. ADAsO reacts with 2 equiv of $MnCp(CO)_2{\cdot}THF$ to form a 2:1 adduct $ADAsO{\cdot}[MnCp(CO)_2]_2$ (eq 1). $ADAsO{\cdot}[MnCp(CO)_2]_2$ has solubility properties similar to $ADSbO{\cdot}[MnCp(CO)_2]_2$ and forms black crystals [mp 165–167 °C

(31) This drawing was made with the KANVAS computer graphics program. This program is based on the program SCHAKAL of E. Keller (Kristallographisches Institute der Universitat Freiburg, FRG), which was modified by A. J. Arduengo, III (E. I. du Pont de Nemours & Co., Wilmington, DE) to produce the back and shadowed planes. The planes bear a 50-pm grid and the lighting source is at infinity so that shadow size is meaningful.

(32) Barbeau, C.; Dichmann, K. S.; Ricard, L. *Can. J. Chem.* **1973**, *51*, 3027.

(dec)] from CH_2Cl_2/hexane. As with the ADSbO adduct, the IR spectrum of ADAsO·$[MnCp(CO)_2]_2$ again shows two pronounced absorptions in the ν_{CO} region [1873 (vs), 1928 (vs), 1950 (sh) cm^{-1}]. The carbonyls attached to the manganese centers exhibit a single resonance in the ^{13}C NMR spectrum at δ 231.1 slightly downfield of their position in the ADSbO adduct. The cyclopentadienyl carbons in ADAsO·$[MnCp(CO)_2]_2$ have a ^{13}C chemical shift of δ 81.7, which is also downfield of the corresponding resonance in the ADSbO adduct (δ 79.7). As observed for the ADSbO adduct, the ^1H and ^{13}C NMR spectra of ADAsO·$[MnCp(CO)_2]_2$ (Table I) suggest an electronic and structural arrangement similar to those of a noncomplexed ring system.[2,4]

Figure 2 illustrates the structure of ADAsO·$[MnCp(CO)_2]_2$ as determined by single-crystal X-ray diffraction. The geometry about the arsenic is quite similar to that observed for the antimony in the ADSbO adduct. However, comparison of Figures 1 and 2 reveals noticeable differences between the structures. The placement of the cyclopentadienyl groups in the two adducts is markedly different. In ADAsO·$[MnCp(CO)_2]_2$ the cyclopentadienyls are synclinal with the tridentate organic ligand. This orientation partially obscures the direct view of the tridentate ligand in Figure 2 but is clearly represented in the shadow on the lower plane. The dihedral angle, N–As–Mn–$Cp_{(centroid)}$, is 14.6°, which is consistent with expectations based on the related arsenidene bis(metal) complexes.[16,25,26,28] The shadow on the lower plane in Figure 2 depicts a planar tridentate organic backbone, as expected from the NMR data (vide supra). The changes in the bond lengths and angles in ADAsO·$[MnCp(CO)_2]_2$ relative to ADAsO follow the same trends observed in the antimony systems. The 11.1 and 9.2% increases in the As–N and As–O bond lengths upon complexation to the manganese centers are even larger than the corresponding changes in the antimony systems. Thus, the arsenic center is also pulled from the tridentate ligand by the manganese centers. The Mn–As–Mn angle (136.6°) is smaller than the corresponding angle in the antimony system but consistent with values observed in arsenidene bis(metal) adducts.[16,25,26,28]

The reaction between $MnCp(CO)_2$·THF and ADPO (eq 2) follows a course different from its heavier analogues. ADPO reacts with only a single equivalent of the manganese electrophile to give a 1:1 adduct, ADPO·$MnCp(CO)_2$. The NMR spectra of ADPO·$MnCp(CO)_2$ suggest a structure for the ADPO fragment that is folded consistent with reactions between ADPO and platinum,[4,6] ruthenium,[10] or iron[33] electrophiles.

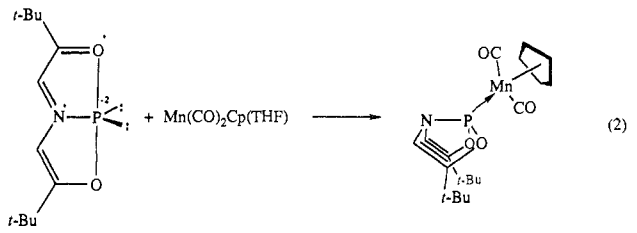

(2)

ADPO **ADPO·$MnCp(CO)_2$**

The tridentate ligand ring protons shift upfield in ADPO·$MnCp(CO)_2$ relative to ADPO (δ 7.50 to 5.74). This shift is consistent with the increase in electron density in the ligand backbone that allows the folding of the ring system to occur. Additionally, the coupling constant for these protons to phosphorus is increased from 9.6 Hz (in ADPO) to 24.3 Hz (in ADPO·$MnCp(CO)_2)_2$). This increase in $^3J_{PH}$ is similar to the results observed in other ADPO metal complexes.[4,6,10] The X-ray structure of ADPO·$MnCp(CO)_2$ is depicted in Figure 3 and shows the expected folded 8-P-4 ADPO ring system.

Discussion

The most striking feature about the ADPnO·$[MnCp(CO)_2]_2$ structures is the fact that the manganese centers are bridged by the pnictogen so that the pnictogen provides one lone pair for each

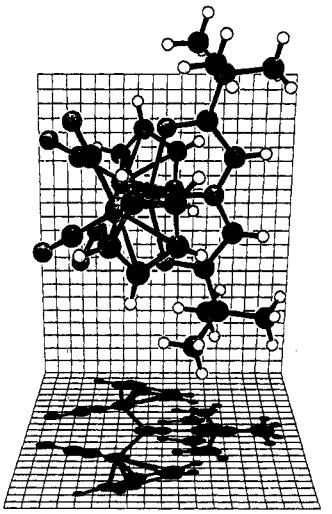

Figure 2. KANVAS[31] drawing of ADAsO·$[MnCp(CO)_2]_2$.

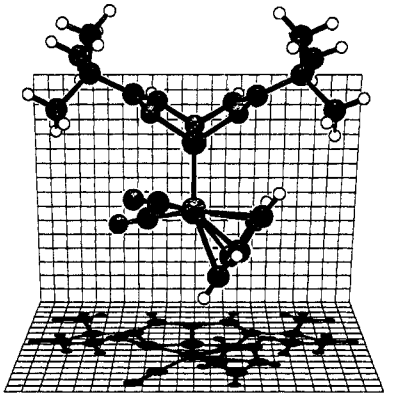

Figure 3. KANVAS[31] drawing of ADPO·$MnCp(CO)_2$.

metal center. These structures clearly demonstrate that both lone pair of electrons at the heavier pnictogen centers of the 10-Pn-3 ADPnO compounds can be chemically reactive. The phosphorus-derived ADPO system shows a different complexation mode in which electronic reorganization of the ADPO ring system occurs. This reorganization results in the formation of a 1:1 adduct in which the phosphorus adopts a tetrahedral 8-electron structure in accord with the octet rule. This result with ADPO is consistent with the previously reported reactions between ADPO and various electrophiles.[4,6,10]

The geometric and NMR spectral changes that occur within the tridentate ligand of ADSbO upon coordination to the manganese centers are similar to the changes observed upon the formation of another 5-coordinate complex, ADSbO·Cl_2.[4] The similarity between the tridentate ligand in these two classes of 5-coordinate antimony compounds is remarkable considering the differences in the type of bonding at the antimony centers. At the time we began the manganese work the only 5-coordinate reference compound available for comparison with the manganese adducts was ADSbO·Cl_2.[4] We decided to synthesize another compound, which would provide more data for comparison and have groups bonded to the antimony that were somewhat different from chlorine. Because of its ease of synthesis (eq 3) and the

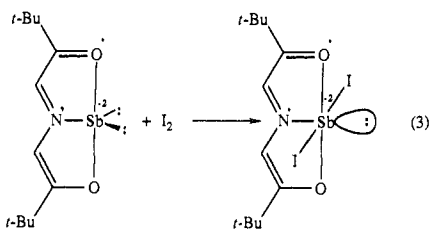

(3)

ADSbO **ADSbO·I_2**

(33) Lattman, M.; Arduengo, A. J., III, unpublished results.

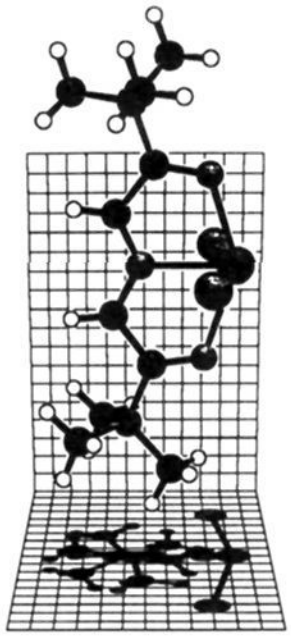

Figure 4. KANVAS[31] Drawing of ADSbO·I_2.

difference in size of chlorine and iodine, the compound we chose to synthesize was ADSbO·I_2. The structure of ADSbO·I_2 as determined by X-ray crystallography is depicted in Figure 4. The multinuclear magnetic resonance data, bond lengths, and bond angles for ADSbO·I_2 are included in Tables I–III, respectively.

There is close resemblance between ADSbO·Cl_2 and ADSbO·I_2. The similarity of the tridentate ligand among these halogen adducts and ADSbO·$[MnCp(CO)_2]_2$ suggests that a large component of the similarity may simply be the result of the increased coordination. Indeed, many of the bond lengths and angles observed in the 4-coordinate antimony compounds $[(ADSbO)_3{\cdot}Ru(C_5(CH_3)_5)]^+$ and $[ADSbO{\cdot}PtCH_3(P(C_6H_5)_3)_2]^+$ are intermediate between the 3-coordinate ADSbO and the 5-coordinate ADSbO derivatives discussed here (Tables II and III). The NMR spectra (Table I) also reflect a trend from 3- to 4- to 5-coordination at the antimony center.

Due to its instability there are no X-ray structural data available for ADAsO·Cl_2.[4] However, the NMR spectral data (Table I) support the type of analogy between ADAsO·Cl_2 and ADAsO·$[Mn(CO)_2Cp]_2$ that is discussed above for their antimony analogues.

Although the similarity between the tridentate ligand backbones in ADSbO·$[MnCp(CO)_2]_2$ and ADSbO·X_2 could possibly be related to the simple fact that these compounds have the same coordination number at antimony, it is important to note that the geometries at the antimony centers are very different. The halogens in the ADSbO·X_2 adducts are bent toward the tridentate ligand while the metal substituents in ADSbO·$[MnCp(CO)_2]_2$ are bent away from the ligand. The bonding at both the metal and halogen adducts of ADPnO sytems can be viewed as "internally solvated" structures, analogous to the representation of the ADPnO systems by the pnictinidene structure **1b**. For the ADPnO bis(metal) adducts structure **5** depicts this conceptual-

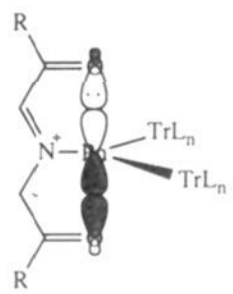

5

Tr = transition metal

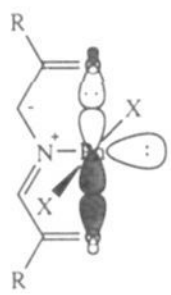

6

X = halogen

ization of an internally solvated pnictinidene bis(metal) adduct. The application of this concept to the halogen adducts produces structure **6**, an internally solvated edge inversion transition state.[34–38]

If structure **5** is considered, the connection between the pnictinidene bis(metal) adducts and the ADPnO bis(metal) adducts is obvious. It is intriguing that the pnictogen–manganese distances and angles are so similar between the pairs of ADPnO·$[MnCp(CO)_2]_2$ and C_6H_5-Pn·$[MnCp(CO)_2]_2$ adducts. The pnictogen–manganese distances are only slightly longer in the ADPnO adducts than the corresponding distances in the phenylpnictinidene adducts. Changes in these distances should be influenced by a reduced $p\pi_{(Pn)}$–$d\pi_{(Mn)}$ bonding interaction in the Mn–Pn–Mn network when the oxygens of the tridentate ligand are in a position to interact with the pnictogen p orbital along the O–Pn–O axis of the ADPnO adducts. Steric factors could also cause a lengthening of these metal–pnictogen bonds. Since both the steric and electronic factors should work in concert to lengthen the Pn–Mn bonds, it is remarkable that these bonds do not show a greater change.

There is a change in the $p\pi_{(Pn)}$–$d\pi_{(Mn)}$ bonding interaction between ADPnO and phenylpnictinidene adducts, which is suggested by the IR spectra of the compounds. The IR spectra of the pnictinidene adducts indicate populations of different Pn–Mn rotamers at ambient temperatures.[16,27,28] The presence of only two strong bands in the ν_{CO} region for ADPnO adducts suggests free rotation about the Pn–Mn bond with little or no barrier. This reduced barrier to rotation of the Pn–Mn bond in the ADPnO adducts relative to C_6H_5–Pn adducts is also supported by the unusual orientation of the cyclopentadienyl groups in ADSbO·$[MnCp(CO)_2]_2$ (vide supra). This orientation does not conform to the usual trend in the pnictinidene·$MnCp(CO)_2$ adducts.[16] Usually the pnictinidene·$MnCp(CO)_2$ adducts show a ~0° or ~180° torsional disposition of the cyclopentadienyl centroid from the unique pnictogen substituent, which places the best $d\pi_{(Mn)}$ *donor orbital in a position to interact with the vacant pnictogen* p-orbital.[16,39] One explanation for the relative insensitivity of the Pn–Mn distance to the degree of the $p\pi_{(Pn)}$–$d\pi_{(Mn)}$ bonding interaction is that the spacial requirements for this type of bond could be the same as for the supporting σ bond between the sp^2 hybridized pnictogen and the manganese centers. The Pn–O hypervalent bonds may also have a fairly flat energy surface for stretching whereas the Pn–Mn bonds have a steeper surface for stretching. The potential flatness of the Pn–O stretching surface is consistent with theoretical models[11] of these types of bonds and in accord with the apparent flexibility of hypervalent bonds in asymmetric environments.[40,41] In light of the flexibility of hypervalent bonding arrays it is not too surprising that the tridentate ligand of the ADPnO molecules shows marked changes in the way it interacts with the central pnictogen when the electronic arrangement of the pnictogen is changed through coordination to metal centers.

There are some subtle changes in Mn–Cp bond distances that seem to reflect the expected electronic changes at the manganese centers of the ADPnO adducts. For ADSbO·$[MnCp(CO)_2]_2$ the Mn–Cp distance is 176.5 pm, which is shorter than the value of 177.2 pm found in ADAsO·$[MnCp(CO)_2]_2$. This change is consistent with the increased electron demand on the Mn–Cp bond by the arsenic center relative to antimony. The change in electron demand may be a result of inherently better $p\pi_{(Pn)}$–$d\pi_{(Mn)}$ overlap between arsenic and manganese centers relative to antimony and manganese centers. The more traditional value of the N–As–Mn–$Cp_{(cent,)}$ dihedral angle relative to the related angle in the ADSbO derivative is in accord with this postulate. Additionally,

(34) Dixon, D. A.; Arduengo, A. J., III; Fukunaga, T. *J. Am. Chem. Soc.* **1986**, *108*, 2461.
(35) Arduengo, A. J., III; Dixon, D. A.; Roe, D. C. *J. Am. Chem. Soc.* **1986**, *108*, 6821.
(36) Dixon, D. A.; Arduengo, A. J., III *J. Am. Chem. Soc.* **1987**, *109*, 338.
(37) Dixon, D. A.; Arduengo, A. J., III *Int. J. Quantum Chem., Quantum Chem. Symp.* **1988**, *No. 22*, 85.
(38) Clotet, A.; Rubio, J.; Illas, F. *J. Mol. Struct. (THEOCHEM)* **1988**, *164*, 351.
(39) Schilling, B. E. R.; Hoffmann, R.; Lichtenberger, D. L. *J. Am. Chem. Soc.* **1979**, *101*, 585.
(40) Gleiter, R.; Gygax, R. *Topics in Current Chemistry*; Springer-Verlag: Berlin, 1976; p 49.
(41) Lozac'h, N. *Advances in Heterocyclic Chemistry*; Academic Press: New York, 1971; p 161.

as would be expected for the pnictinidene complexes, the Mn–Cp distance of 179.0 pm for C_6H_5–As·$[MnCp(CO)_2Cp]_2$ is the largest value listed for this parameter in Table II. The theoretical descriptions of the bonding arrangements in these metal adducts are presently being developed in our laboratory and should contribute to our understanding of these systems.

The interesting similarities between the spectral and structural properties of the tridentate organic ligand in different 5-coordinate adducts of the ADPnO molecules still remain. These similarities occur in spite of the very different coordination geometries of the ADPnO·X_2 and ADSbO·$[MnCp(CO)_2]_2$ adducts. It is tempting to account for these similarities in terms of the coordination number at the pnictogen, but it does not seem reasonable to expect such similarities when the electronic and structural arrangements at the pnictogen centers are so different. One common feature between the pnictogen centers of the ADPnO·X_2 and ADSbO·$[MnCp(CO)_2]_2$ adducts is that the π interactions between the central pnictogen and the ligand backbone are somewhat blocked by the "new" substituents (halogen or manganese). This should induce similar changes in the two types of bis(adducts) relative to the initial ADPnO molecules. Structure **6** depicts an internally solvated edge inversion transition state for an R–PnX_2 species (R in this case is the azomethine ylide). Just as structure **5** illustrated an internally solvated pnictinidene bis(metal) adduct in which the pnictinidene/metal fragment was little changed from noncomplexed references, the edge inversion transition state in **6** is exactly what would be expected based on theoretical models.[36,38] The Sb–Cl bonds in ADSbO·Cl_2 are 7.8% longer than in $SbCl_3$.[42] The Sb–I bonds in ADSbO·I_2 are 10.5% longer than in SbI_3.[42] These increases are typical of those expected for the formation of the X–Sb–X hypervalent array and are in accord with theoretical calculations on other pnictogen trihalide edge inversion processes.[36,38]

Conclusions

The synthesis and characterization of the ADPnO·$[MnCp(CO)_2]_2$ compounds (Pn = As or Sb) demonstrate the chemical reactivity of both lone pairs of electrons at the pnictogen centers of the corresponding ADPnO compounds. The formation of the 1:1 adduct, ADPO·$MnCp(CO)_2$, as opposed to the 2:1 adducts observed with the heavier pnictogens demonstrates the close energetic relationship between the planar 10-P-3 ADPO ground state and the folded 8-P-3 ADPO structure. This phosphorus result is in accord with other ADPO coordination chemistry and theoretical expectations.

There is a close structural analogy between the Pn$[MnCp(CO)_2]_2$ fragments in the ADPnO adducts and the pnictinidene bis(manganese) compounds. The most significant difference appears to be the lower Pn–Mn rotational barrier in the ADPnO adducts. This reduced rotational barrier is probably the result of a diminished $p\pi_{(Pn)}$–$d\pi_{(Mn)}$ bonding interaction as a result of persistent interactions between the pnictogen center and the oxygens of the tridentate ligand.

As oxidative additions and coordination chemistry take place at the central pnictogen of the ADPnO molecules, the flexibility of the 3-center 4-electron hypervalent bond allows the formation of compounds with similar structural and NMR spectral properties in tridentate organic ligand. Thus, ADPnO·X_2 compounds are quite similar to ADPnO·$[MnCp(CO)_2]_2$ compounds. This gives rise to an apparent relation between coordination number at the central pnictogen and the properties of the tridentate ligand.

Experimental Section

Reactions and manipulations were carried out under an atmosphere of dry nitrogen, either in a Vacuum Atmospheres drybox or using standard Schlenk techniques. Although the products turned out to be light stable, all procedures were carried out with minimum exposure to light. Solvents were dried (using standard procedures),[43] distilled, and deoxygenated prior to use, unless otherwise indicated. Glassware was oven-dried at 160 °C overnight. The photochemical apparatus (Ace Glass No. 7861-245) consisted of a medium-pressure Conrad-Hanovia mercury-vapor lamp (450 W) inserted into a standard immersion well reaction vessel (250-mL capacity). External cooling was accomplished by inserting the vessel into a cold bath. The reaction mixture was magnetically stirred and nitrogen continuously bubbled through the solution during the photolysis. IR spectra were recorded on a Perkin-Elmer 983G infrared spectrophotometer. ^1H NMR spectra were recorded on a General Electric QE-300 spectrometer. ^{13}C and ^{31}P NMR spectra were recorded on a Nicolet NT-300WB spectrometer. NMR references are $(CH_3)_4Si$ (^1H, ^{13}C), 85% H_3PO_4 (^{31}P), and $NH_4^+NO_3^-$ (^{14}N, ^{15}N). Mass spectra were obtained on a VGMM 7070 double-focusing high-resolution mass spectrometer. Melting points were obtained on a Thomas-Hoover capillary apparatus and are uncorrected. Elemental analyses were performed by Oneida Research Services, Whitesboro, NY.

Cyclopentadienylmanganese tricarbonyl was purchased commercially and used without further purification, and the ADPnO derivatives were synthesized as described previously.[4]

ADSbO·$[MnCp(CO)_2]_2$. A photochemical apparatus was charged with a solution of $MnCp(CO)_3$ (1.00 g, 4.90 mmol) in THF (250 mL) and irradiated for 3.5 h, keeping the internal temperature between −32 and +40 °C. The solution turned wine-red, indicating formation of $MnCp(CO)_2$·THF. The stirred reaction mixture was then immersed in a −78 °C bath and treated with a solution of ADSbO (0.665 g, 2.00 mmol) in THF (15 mL). The reaction was allowed to warm to 0 °C over 2 h and stirred at this temperature for another 16 h. The volatiles were then pumped off and the residue was recrystallized (without heating) from CH_2Cl_2/hexane (two crops), yielding dark green rodlike air-sensitive crystals of ADSbO·$[MnCp(CO)_2]_2$: 0.979 g (72%); mp 218–220 °C (dec). Mass spectrum (EI): molecular ion m/z 683 (8%), base peak m/z 265 ($C_{12}H_{20}NO_2Mn^+$). NMR spectra: ^1H (CD_2Cl_2), δ 1.31 (s, *t*-Bu, 18 H), 4.50 (s, Cp, 10 H), 8.08 (s, NCH, 2 H); $^{13}C\{^1H\}$ (CD_2Cl_2), δ 27.6 (s, CH_3), 41.0 (s, $C(CH_3)_3$), 79.7 (s, Cp), 119.9 (s, CN), 196.5 (s, COP), 229.3 (br s, MnCO). IR spectrum (cm^{-1}, THF): 1865 (vs), 1919 (vs), 1932 (sh). Anal. Calcd for $C_{26}H_{30}NMn_2O_6Sb$: C, 45.65; H, 4.42; N, 2.05. Found: C, 45.67; H, 4.40; N, 1.93.

ADAsO·$[MnCp(CO)_2]_2$. In a procedure similar to the one above, a solution of $MnCp(CO)_3$ (0.500 g, 2.45 mmol) in THF (275 mL) was irradiated for 2 h, followed by treatment with ADAsO (0.279 g, 0.978 mmol). After overnight stirring at 0 °C, the IR spectrum indicated the presence of some of the $MnCp(CO)_2$·THF complex. The reaction was then stirred for another 3 h at ambient temperature. Similar workup yielded black air-sensitive crystals of ADAsO·$[MnCp(CO)_2]_2$: 0.119 g (19%); mp 165–167 °C (dec). NMR spectra: ^1H (CD_2Cl_2), δ 1.32 (s, *t*-Bu, 18 H), 4.49 (s, Cp, 10 H), 7.80 (s, NCH, 2 H); $^{13}C\{^1H\}$ (CD_2Cl_2), δ 27.4 (s, CH_3), 40.3 (s, $C(CH_3)_3$), 81.7 (s, Cp), 118.7 (s, CN), 191.5 (s, COP), 231.1 (br s, MnCO). IR spectrum (cm^{-1}, THF): 1873 (vs), 1928 (vs), 1950 (sh). Anal. Calcd for $C_{26}H_{30}NMn_2O_6As$: C, 49.00; H, 4.74; N, 2.20. Found: C, 48.13; H, 4.72; N, 1.49.

ADPO·$MnCp(CO)_2$. In a procedure similar to those described above, a solution of $MnCp(CO)_3$ (1.00 g, 4.90 mmol) in THF (250 mL) was irradiated for 3.5 h, followed by treatment with ADPO (0.483 g, 2.00 mmol). After overnight stirring at 0 °C, the IR spectrum indicated the presence of a $MnCp(CO)_2$ fragment [ν_{CO} (cm^{-1}): 1900 (vs), 1962 (vs)], as well as $MnCp(CO)_3$. The volatiles were then pumped off and an NMR spectrum (THF-d_8) was taken of the crude material: ^1H, δ 1.11 (s, *t*-Bu, 18 H), 4.62 (s, Cp, 5 H), 5.83 (d, $^3J_{PH}$ = 24.0 Hz, NCH, 2 H); $^{31}P\{^1H\}$, δ 256 (br). Some $MnCp(CO)_3$ was also present. The product was not isolated. A similar reaction using an approximate 1:1 molar ratio of reactants led to the same product.

A THF solution (250 mL) of $MnCp(CO)_3$ (0.500 g, 2.45 mmol) was photolyzed at −35 °C for 3 h to produce a wine-red solution. To this solution was added ADPO (0.483 g, 2.00 mmol) in THF (20 mL) at 0 °C. The mixture was allowed to warm to room temperature and was stirred overnight at 23 °C. The resulting brown-orange solution was evaporated under vacuum, and the residue was extracted into hexane, filtered, and concentrated to obtain 0.290 g of ADPO·$MnCp(CO)_2$ (35%) as yellow crystals, mp 101–104 °C. NMR spectra: ^1H (CD_2Cl_2) δ 1.12 (s, 18 H, *t*-Bu), 4.62 (d, J_{HP} = 1.9 Hz, 5 H, Cp), 5.74 (d, $^3J_{HP}$ = 24.3 Hz, 2 H, NCH); ^{13}C (CD_2Cl_2) δ 27.4 (s, CH_3), 32.5 (d, J_{PC} = 4.6 Hz, C_4C), 81.7 (s, Cp), 113.3 (d, J_{PC} = 1.1 Hz, NC), 155.2 (d, J_{PC} = 5.4 Hz), 228 (br). $^{31}P\{^1H\}$ (CD_2Cl_2) δ 256. Anal. Calcd for $C_{19}H_{25}NMnO_4P$: C, 54.68; H, 6.04; N, 3.36. Found: C, 54.72; H, 6.13; N, 3.27.

ADSbO·I_2. In a drybox, under a nitrogen atmosphere, a 50-mL round-bottom flask, equipped with a magnetic stir bar, was charged with 20 mL of CH_2Cl_2 and ADSbO (1.0 g, 3.0 mmol). The flask and its

(42) *CRC Handbook of Chemistry and Physics*; Chemical Rubber Publishing Co.: Boca Raton, FL, 1986–1987.

(43) Perrin, D. D.; Armarego, W. L. F.; Perrin, D. R. *Purification of Laboratory Chemicals*; Pergamon: New York, 1985.

contents were cooled to -25 °C. A suspension of 0.76 g of I_2 (3.0 mmol) in 20 mL of CH_2Cl_2 was added dropwise while the reaction mixture was stirred vigorously. After the addition was complete, the mixture was stirred for 2 h at -25 °C. The CH_2Cl_2 was removed in vacuo. The crude solids were recrystallized from CH_2Cl_2/hexane to give 1.26 g (71%) of ADSbO·I_2 as black needles; mp 220-222 °C. A second crop (0.48 g; 27% of product was recovered from concentration of the mother liquors. First crop ^1H NMR: (CD_2Cl_2) δ 1.36 (s, *t*-Bu, 18 H), 8.12 (s, NCH, 2 H). ^{13}C NMR (CD_2Cl_2) δ 26.59 (s, CH_3), 41.25 (s, $C(CH_3)_3$), 121.76 (s, CN), 203.79 (s, CO). ^{14}N NMR (CD_2Cl_2) δ -63. Anal. Calcd for $C_{12}H_{20}NO_2SbI_2 \cdot CH_2Cl_2$: C, 23.26; H, 3.28; N, 2.08. Found: C, 23.08; H, 2.91; N, 1.99.

X-ray Crystal Structure of ADSbO·[MnCp(CO)$_2$]$_2$: Formula, $C_{26}H_{30}NO_6SbMn_2$ monoclinic; space group $C2/c$ (No. 15); a = 1869.9 (2), b = 1559.6 (3), c = 945.5 (1) pm; β = 92.47 (1)°; T = -70 °C; Z = 4; FW = 684.16; D_c = 1.649 g/cm^3; μ(Mo) = 18.85 cm^{-1}. Crystal description: black, parallelopiped (0.20 × 0.15 × 0.30 mm) grown by cooling a CH_2Cl_2/hexane solution of ADSbO·[MnCp(CO)$_2$]$_2$. A total of 4354 reflections were collected, 2.2° ≤ 2θ ≤ 55.0°, on a Enraf-Nonius CAD4 diffractometer with graphite monochromator using MoKα radiation (λ = 71.073 pm). With 1948 unique reflections of intensity greater than 3.0σ, the structure was solved by automated Patterson analysis (PHASE) and standard difference Fourier techniques. All non-hydrogen atoms were refined with anisotropic thermal parameters. All hydrogens were placed in calculated positions. The final R factors were R = 0.046, R_w = 0.038. The final difference Fourier showed the largest residual density to be 0.47 e/Å^3, near the manganese carbonyl carbon, which is synclinal to the tridentate ligand. Atomic coordinates, bond lengths, bond angles, thermal parameters, and additional details are available in supplementary material.

X-ray Crystal Structure of ADAsO·[MnCp(CO)$_2$]$_2$: formula, $C_{26}H_{30}NO_6AsMn_2$ monoclinic; space group $C2/c$ (No. 15); a = 1827.2 (3), b = 1216.0 (3), c = 1197.2 (3) pm; β = 90.35 (1)°; T = -100 °C; Z = 4; FW = 637.33; D_c = 1.591 g/cm^3; μ(Mo) = 21.83 cm^{-1}. Crystal description: black, parallelogram (0.36 × 0.21 × 0.50 mm) grown by cooling a CH_2Cl_2/hexane solution of ADAsO·[MnCp(CO)$_2$]$_2$. A total of 3376 reflections were collected, 4.0° ≤ 2θ ≤ 55.0°, on a Syntex R3 diffractometer with graphite monochromator using Mo Kα radiation (λ = 71.073 pm). With 2507 unique reflections of intensity greater than 3.0σ, the structure was solved by automated Patterson analysis (PHASE) and standard difference Fourier techniques. All non-hydrogen atoms were refined with anisotropic thermal parameters. All hydrogens were placed in calculated positions. The final R factors were R = 0.025, R_w = 0.029. The final difference Fourier showed the largest residual density to be 0.19 e/Å^3, near the manganese. Atomic coordinates, bond lengths, bond angles, thremal parameters, and additional details are available in supplementary material.

X-ray Crystal Structure of ADPO·MnCp(CO)$_2$: formula, $C_{19}H_{25}NO_4PMn$ triclinic; space group $P\bar{1}$ (No. 2); a = 916.7 (1), b = 941.5 (3), c = 1280.4 (2) pm; α = 91.15 (2)°, β = 103.66 (1)°, γ = 106.15 (2)°; T = -70 °C; Z = 2; FW = 417.33; D_c = 1.349 g/cm^3; μ(Mo) = 7.14 cm^{-1}. Crystal description: pale yellow, irregular block (0.42 × 0.34 × 0.50 mm) grown by cooling a hexane solution of ADPO·MnCp(CO)$_2$. A total of 3722 reflections were collected, 3.3° ≤ 2θ ≤ 50.0°, on a Enraf-Nonius CAD4 diffractometer with graphite monochromator using MoKα radiation (λ = 71.073 pm). With 2956 unique reflections of intensity greater than 3.0σ, the structure was solved by automated Patterson analysis (PHASE) and standard difference Fourier techniques. All non-hydrogen atoms were refined with anisotropic thermal parameters. All hydrogens were placed in calculated positions and refined. The final R factors were R = 0.029, R_w = 0.036. The final difference Fourier showed the largest residual density to be 0.32 e/Å^3, near the phosphorus. Atomic coordinates, bond lengths, bond angles, thermal parameters, and additional details are available in supplementary material.

X-ray Crystal Structure of ADSbO·I$_2$: formula, $C_{12}H_{20}NO_2SbI_2 \cdot CH_2Cl_2$ monoclinic; space group $P2_1/n$ (No. 14); a = 1015.7 (4), b = 1013.7 (3), c = 2107.1 (7) pm; β = 98.05 (1)°; T = 23 °C; Z = 4; FW = 670.78; D_c = 2.07 g/cm^3; μ (Mo) = 43.92 cm^{-1}. Crystal description: black, trapezoid (0.23 × 0.15 × 0.48 mm) grown by cooling a toluene solution of ADSbO·I_2·(CH_2Cl_2). A total of 4812 reflections were collected, 2.0° ≤ 2θ ≤ 53.0°, on a Enraf-Nonius CAD4 diffractometer with graphite monochromator using MoKα radiation (λ = 71.073 pm). After absorption corrections (DIFABS), there were 3496 unique reflections of intensity greater than 3.0σ. The initial atomic coordinates were taken from a room-temperature structure determination with another crystal. All non-hydrogen atoms were refined with anisotropic thermal parameters. All hydrogens were placed in calculated positions and refined. Anomalous dispersion terms were included for iodine and antimony. The final R factors were R = 0.027, R_w = 0.027. The final difference Fourier showed the largest residual density to be 0.62 e/Å^3 near one of the iodines. Atomic coordinates, bond lengths, bond angles, thermal parameters, and additional details are available in supplementary material.

Acknowledgment is made to Dr. C. A. Stewart for helpful discussions. The excellent technical assistance of J. E. Feaster, Jr., and H. A. Craig made much of this work possible.

Supplementary Material Available: A complete description of the X-ray crystallographic structure determinations on ADSbO·[MnCp(CO)$_2$]$_2$, ADAsO·[MnCp(CO)$_2$]$_2$, ADPO·MnCp(CO)$_2$, and ADSbO·I_2 including experimental procedures, tables of data, and ORTEP structure drawings (20 pages). Ordering information is given on any current masthead page.

Photochemistry of Dipeptides in Aqueous Solution

Roger R. Hill,* John D. Coyle,† David Birch, Edwin Dawe, Graham E. Jeffs, David Randall, Iwan Stec, and Tessa M. Stevenson

Contribution from the Department of Chemistry, The Open University, Milton Keynes MK7 6AA, United Kingdom. *Received June 26, 1990*

Abstract: The photochemical lability of peptides is poorly understood, largely because of the lack of product data. In the present study, product analyses have been carried out following the photolyses in aqueous solution of selected glycyl dipeptides (Gly-Gly, DL-Ala-Gly, L-Val-Gly, L-Pro-Gly, L-Phe-Gly, and Gly-L-Phe), L-prolyl-L-phenylalanine, and L-phenylalanyl-L-proline. Efficient deamination and decarboxylation of aliphatic dipeptides generate thermal precursors of simple amides in a photoinduced electron-transfer process involving the peptide bond. An analogous pathway in the photodegradation of phenylalanyl peptides suffers competition from other types of reaction.

Proteins play an important but ill-defined role in virtually all photobiological processes and are significant targets in biological photodamage. Absorption of solar radiation by prosthetic pigments or aromatic side chains often initiates chemistry remote from the chromophore, but the part played by peptide bonds in such processes remains obscure. The assumption that it is wholly structural, imposing only order and direction, is questionable given, for example, the ready one-electron reduction of peptide groups[1-3] and

† Present address: Cookson Group plc, Sandy Lane, Yarnton, Oxford OX5 1AF, U.K.

(1) Kayushin, L. P.; Ilyasova, V. P.; Azizova, O. A. *Stud. Biophys.* **1978**, *49*, 187-198.

0002-7863/91/1513-1805$02.50/0